Sub-cellular description of cardiac action potential propagation with gap junctions dynamics

Jean Bragard
Department of Physics & Applied Mathematics,
School of Sciences,
University of Navarra. 31008 Pamplona. SPAIN.

Dynamics Days, Naples, 6th of September 2023

Why are we interested in studying **cardiac dynamics** ?

Rank[1]	Cause of death (based on ICD–10, 1992)	Number	Percent of total deaths	2005 crude death rate
...	All causes	2,448,017	100.0	825.9
1	Diseases of heart (I00–I09,I11,I13,I20–I51)	652,091	26.6	220.0
2	Malignant neoplasms (C00–C97)	559,312	22.8	188.7
3	Cerebrovascular diseases (I60–I69)	143,579	5.9	48.4
4	Chronic lower respiratory diseases (J40–J47)	130,933	5.3	44.2
5	Accidents (unintentional injuries) (V01–X59, Y85–Y86)	117,809	4.8	39.7
6	Diabetes mellitus (E10–E14)	75,119	3.1	25.3
7	Alzheimer's disease (G30)	71,599	2.9	24.2
8	Influenza and pneumonia (J10–J18)	63,001	2.6	21.3
9	Nephritis, nephrotic syndrome and nephrosis (N00–N07,N17–N19,N25–N27)	43,901	1.8	14.8
10	Septicemia (A40–A41)	34,136	1.4	11.5
11	Intentional self-harm (suicide) (*U03, X60–X84, Y87.0)	32,637	1.3	11.0
12	Chronic liver disease and cirrhosis (K70, K73–K74)	27,530	1.1	9.3
13	Essential (primary) hypertension and hypertensive renal disease (I10,I12)	24,902	1.0	8.4
14	Parkinson's disease (G20–G21)	19,544	0.8	6.6
15	Assault (homicide) (*U01–*U02, X85–Y09, Y87.1)	18,124	0.7	6.1
...	All other causes (residual)	433,800	17.7	146.4

Cardiac diseases are among the leading causes of death and
we should understand better all the mechanisms associated with them.

Normal electric activity may be disrupted by failures in the propagation of the action potentials

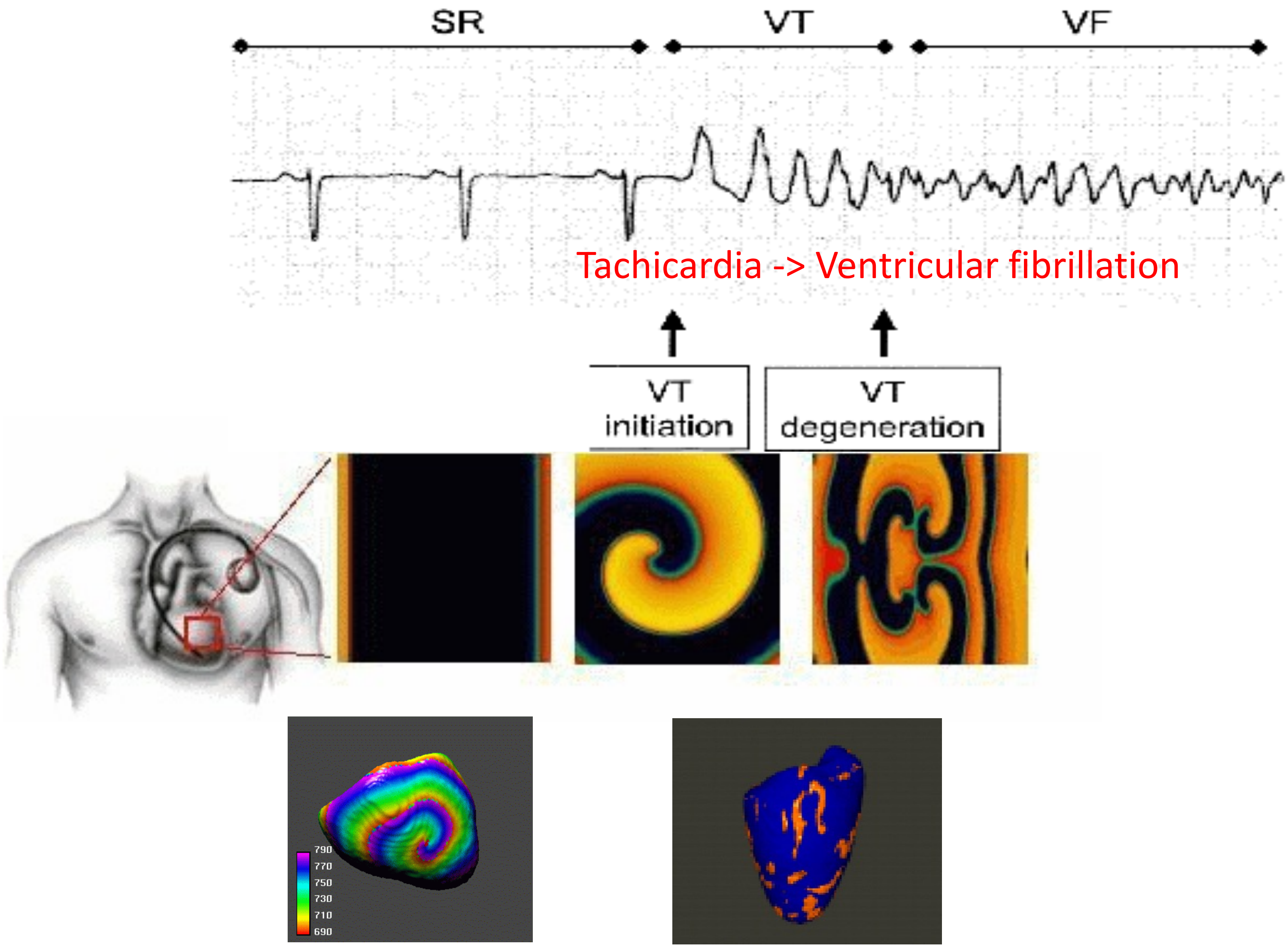

(Keener y Panfilov (1995))

The structure of the cardiac muscle is complex and influences its electrical behavior and dynamics

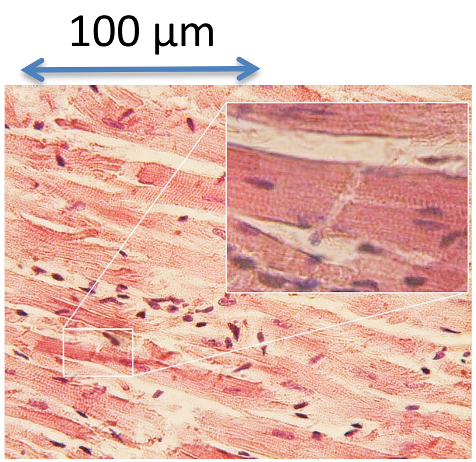

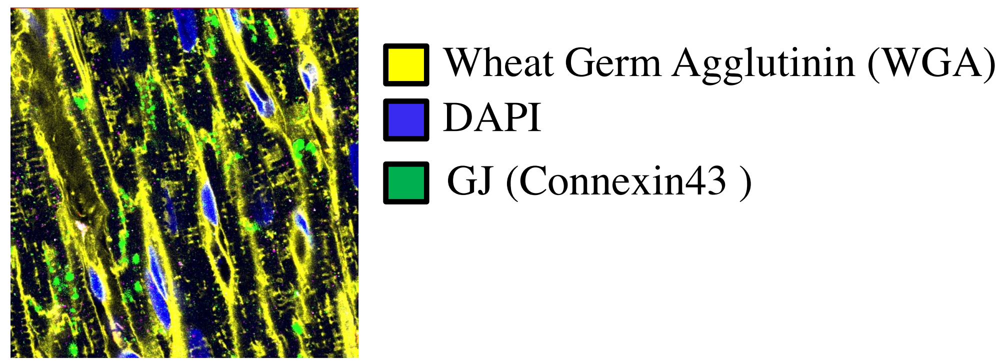

The cardiac muscle is formed with cardiomyocytes, gap junctions (GJ), collagen and elastin fibers, fibroblasts, blood vessels,…

Sources : Wikipedia; Sachse's lab.

Gap junctions (GJ) are essential for the propagation of the electrical impulse AP from one myocyte to the next.

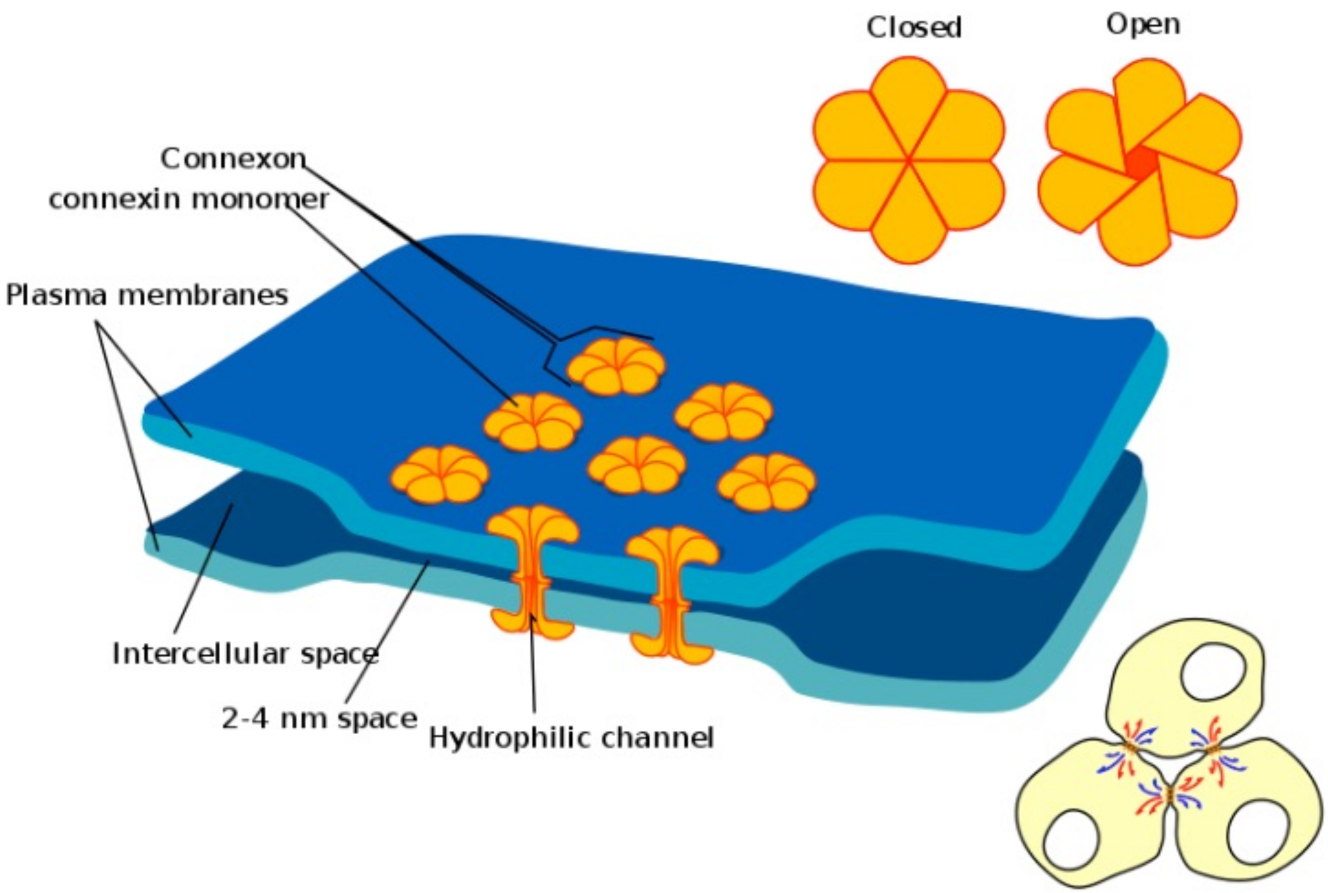

GJs form low electrical resistance passages between cardiomyocytes.

Source : Wikipedia

Different types of gap junctions (GJ) have been identified in the cardiac muscle

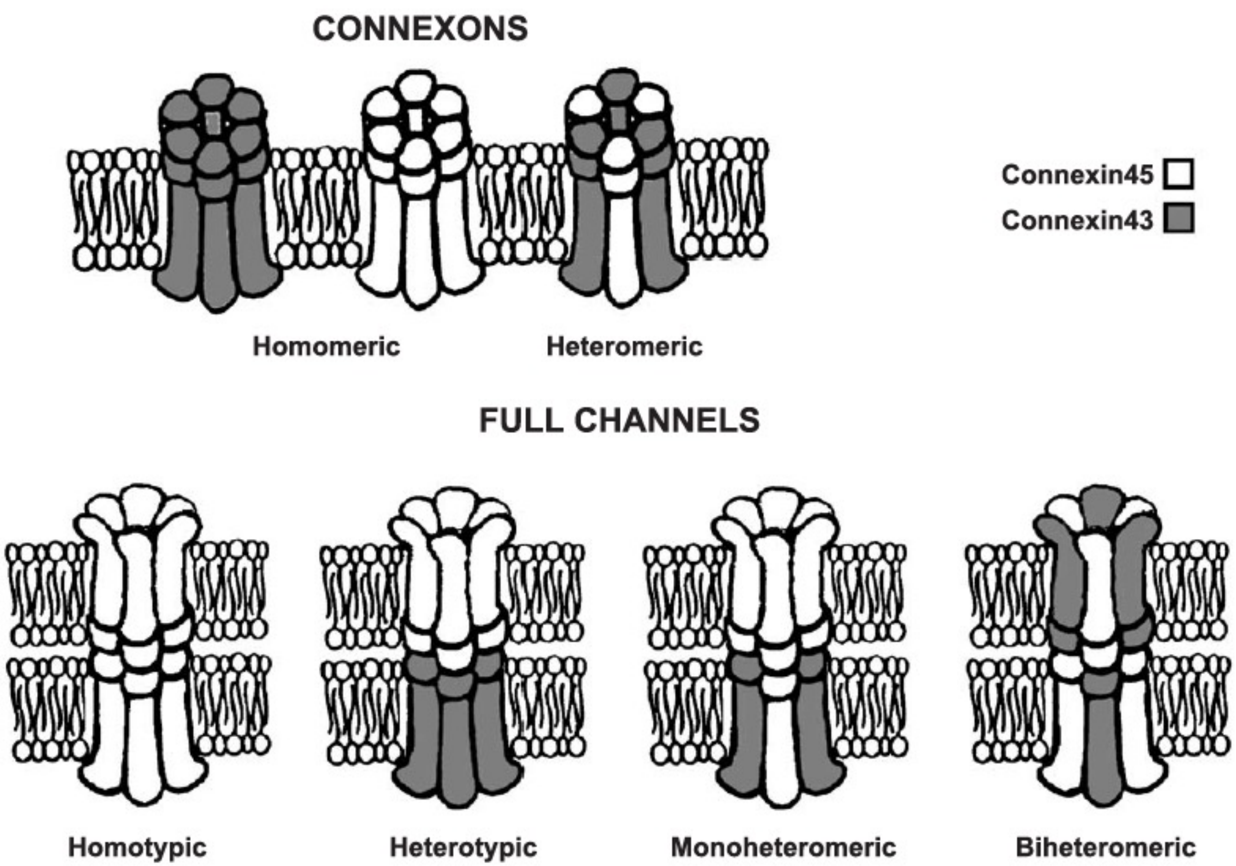

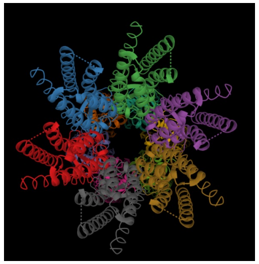

Cx46 (PDB)

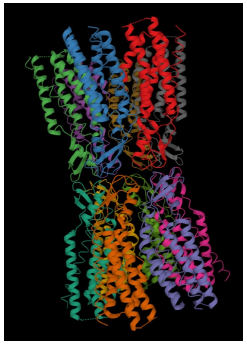

In cardiac tissue of mammalian, connexins type Cx40, Cx43 and Cx45 are the most common.

The permeability of the GJ depends on its structure (g approx. 10 to 300 pS)

Source : AP Moreno, Cardiovasc. Res. **62** , 2004

Different types of gap junctions (GJ) have been identified in the cardiac muscle (II)

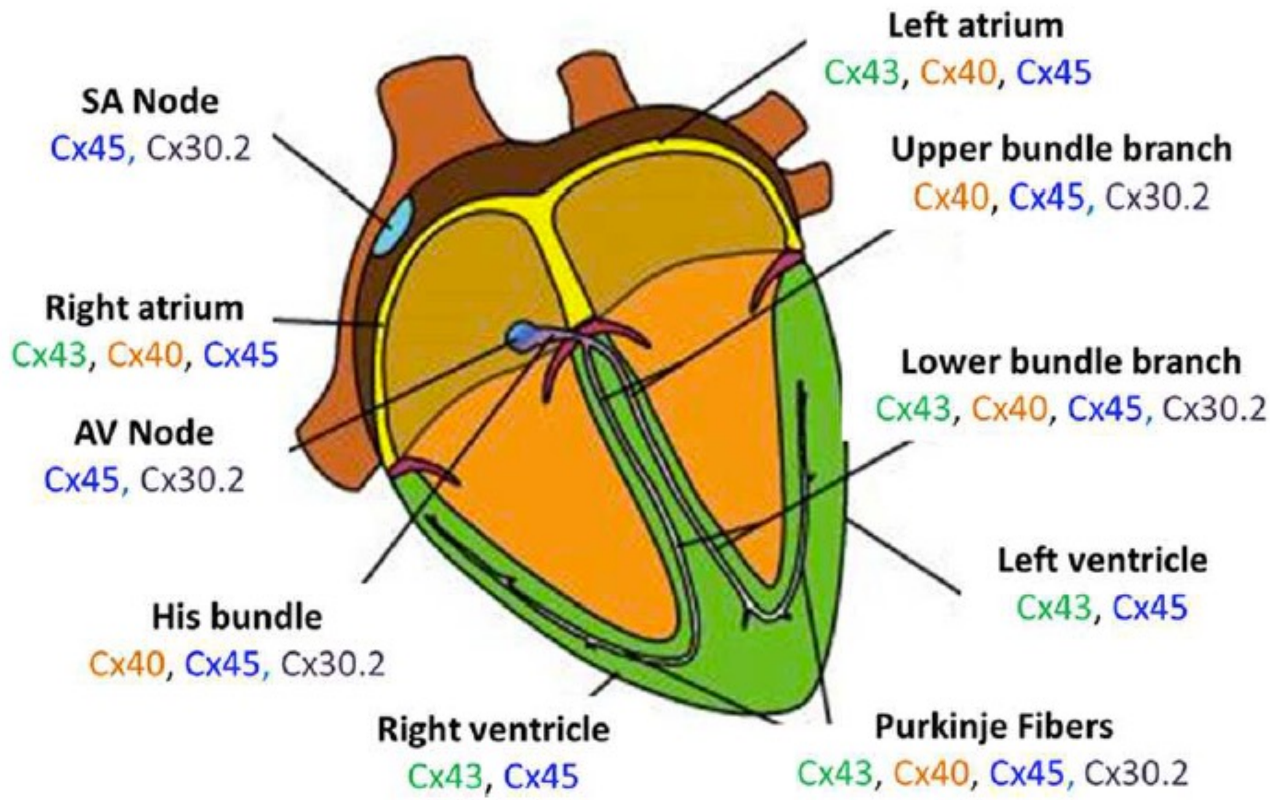

The connexin's expression pattern varies in different location of the heart

Source : T. Desplantez et al., BMC Cell Biol. **18** , 2017

Dual voltage-clamp method and whole-cell recording allow to measure the electrical properties of the GJ

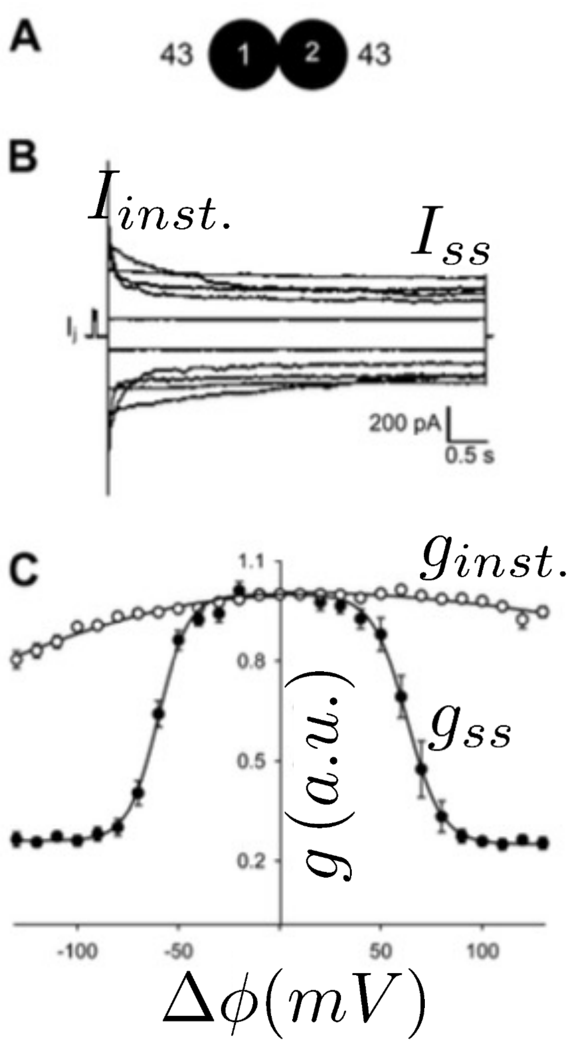

a) Fix the membrane potential of both cells

$$\Delta\phi = V_2 - V_1 \qquad \text{transjunctional voltage}$$

b) Measure the current between cells

$$I_{inst.} \qquad\qquad I_{ss}$$

c) Calculate the normalized conductances

$$g_{inst.} = I_{inst.}/\Delta\phi \quad \sim 100\,pS$$

$$g_{ss} = I_{ss}/\Delta\phi$$

The conductance between the two cells is a dynamical variable

Source : T. Desplantez et al., Eur. J. Physiol. **448** , 2004

Mathematical model of a strand of cardiac tissue

Myocyte (i) Myocyte (i+1)

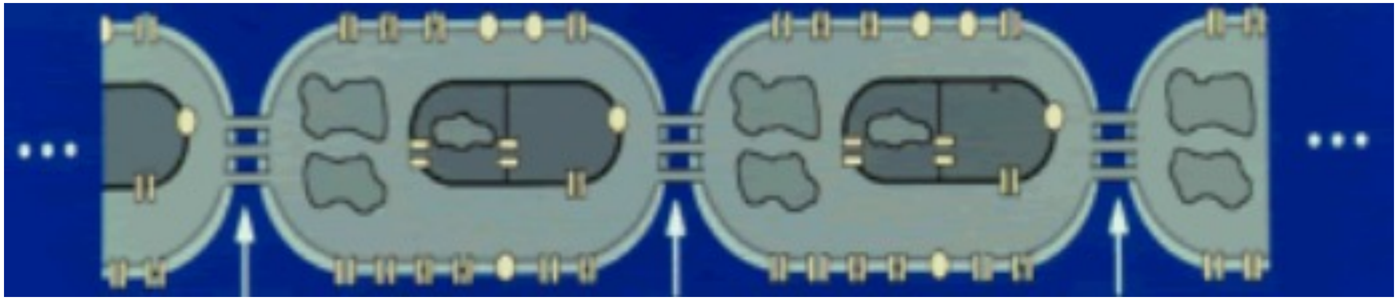

g (i-1) g (i) g (i+1)

1) Gap Junction's dynamics

$$\frac{dg_i}{dt} = \frac{g_{ss}(\Delta\phi_i) - g_i}{\tau_g(\Delta\phi_i)}$$

$$\Delta\phi_i = V_{i+1} - V_i$$

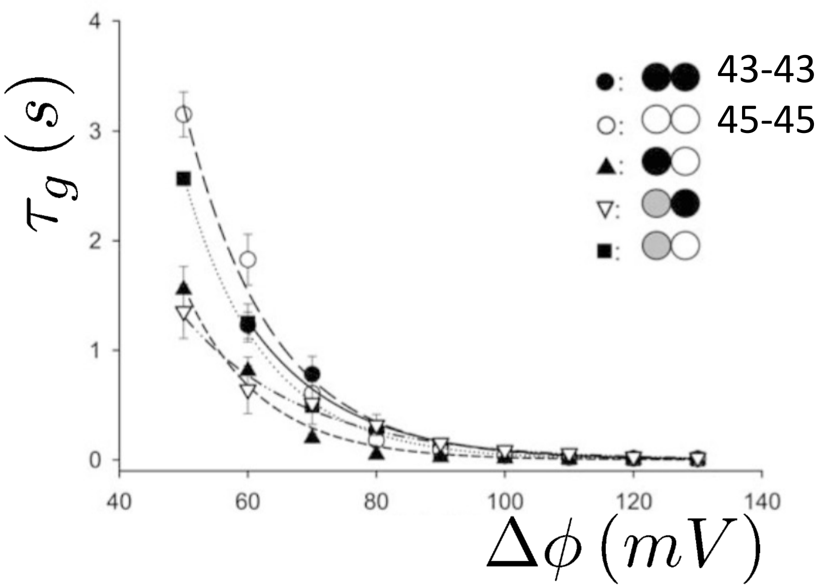

The time constant τ_g is highly dependent of the connexin's transjunctional voltage

Source : T. Desplantez et al., Eur. J. Physiol. **448** , 2004

Mathematical model of a strand of cardiac tissue (ii)

Myocyte (i) Myocyte (i+1)

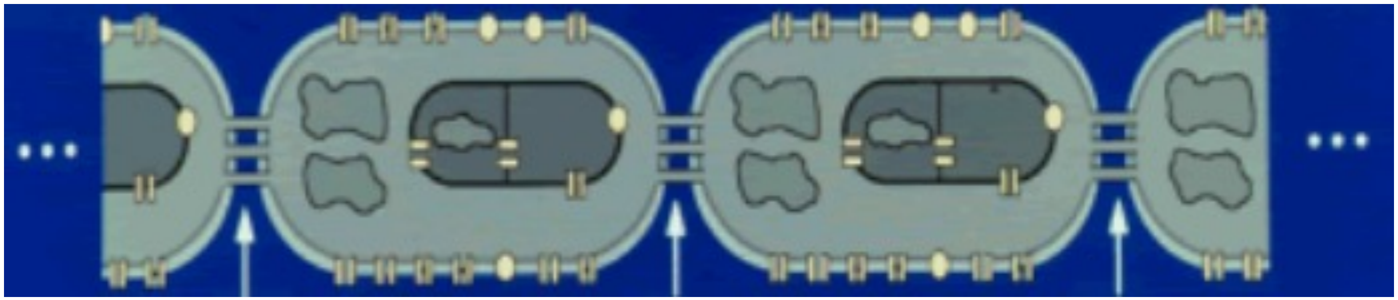

g (i-1) g (i) g (i+1)

2) Myocyte's transmembrane dynamics

$$\frac{\partial V}{\partial t} + \frac{I_{myo} + I_{ext}}{\mathcal{C}} = \nabla \cdot (D \nabla V)$$

$$\frac{\partial \mathbf{s}}{\partial t} = f(V, \mathbf{s})$$

5 variables model (BCN)

$$V = \phi_{intra} - \phi_{extra}$$

Monodomain approximation

$$D(x,t) = \bar{D}\, g(x,t)$$

$$\bar{D} = 1.5\,\mathrm{cm}^2/\mathrm{s}$$

- The gap junctions are the primary sites of membrane potential changes
- The entire myocyte cytoplasm becomes effectively iso-potential.

Sources : Y. Rudy, Circ. Res. 1997; Cantalapiedra et al. PRE **82** 2010.

Numerical method

Myocyte (i) Myocyte (i+1)

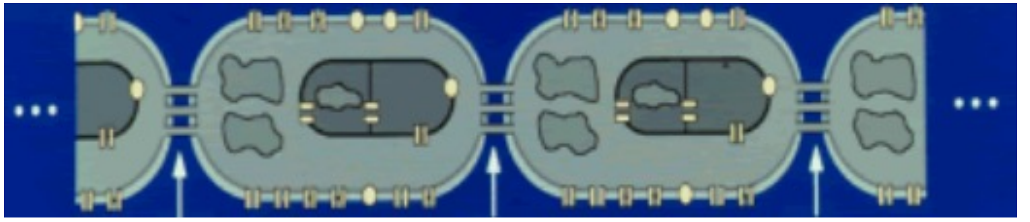

g (i-1) g (i) g (i+1)

$$\delta x = 100\mu\text{m}$$

$$V_i^{(n+1)} = V_i^{(n)} + \bar{D}\frac{\delta t}{\delta x^2}\left\{g_i^{(n)}\left[V_{i+1}^{(n)} - V_i^{(n)}\right] - g_{i-1}^{(n)}\left[V_i^{(n)} - V_{i-1}^{(n)}\right]\right\} - \delta t\,\frac{I_{myo}^{(n)} + I_{ext}^{(n)}}{\mathcal{C}}$$

$\delta t = 10\mu\text{s}$ Integration time step

$$g_i^{(n+1)} = g_i^{(n)} + \delta t\,\frac{g_{ss}(\Delta\phi_i^{(n)}) - g_i^{(n)}}{\tau_g(\Delta\phi_i^{(n)})}$$

Super-index (n) refers to time step n. Subscript i refers to position i in the chain.

Source : Keener 1991

Numerical method (Sub-cellular scale)

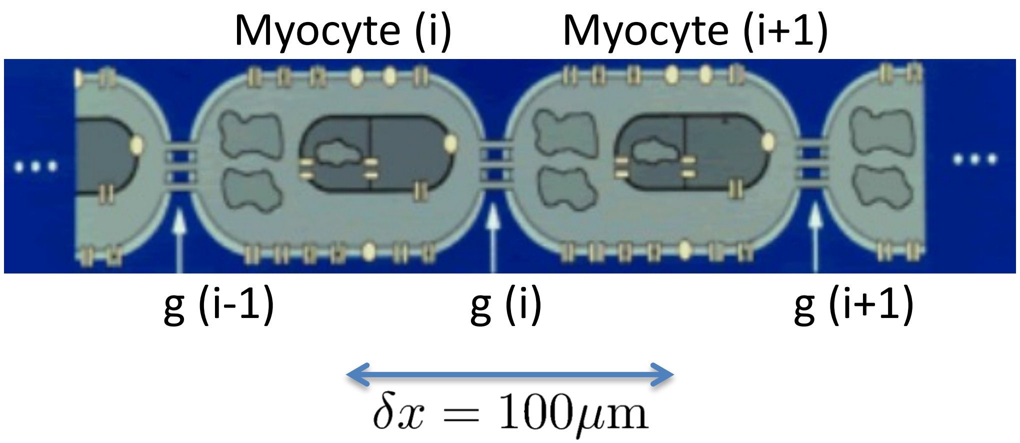

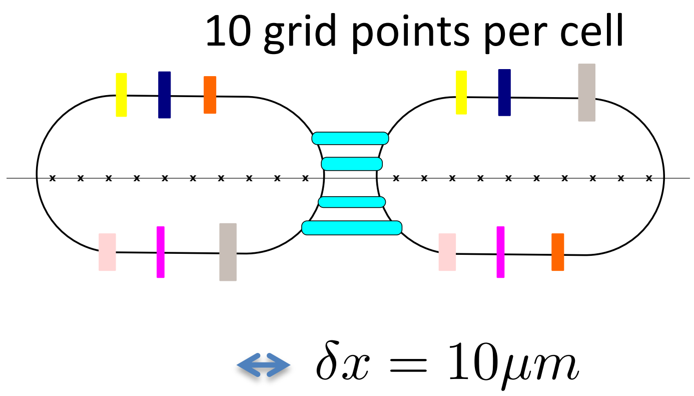

$$FD = \frac{D_{intra}}{D_{gap}}$$

For the sub-cellular simulations, the Euler explicit is modified to

an implicit scheme (first and second order in time) to ensure numerical stability,

Also, we now have two diffusion parameters (regular: intracellular and gap diffusion).

Stimulation protocol (L=400 cells)

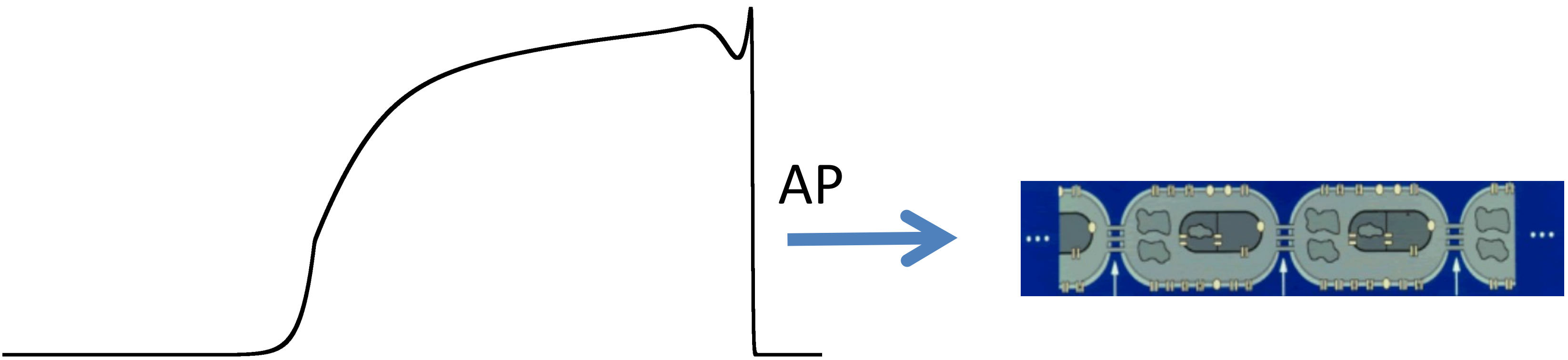

i = 1 … 400

1. Same initial values are set to all the GJ conductances ($g_i = g_{ini}$)
2. We excite the first 7 cells (i=1..7) to elicit an AP that propagates through the fiber
3. We repeat the stimulation with a period of T = 480 ms
4. We measure the time evolution of the GJ conductances after each stimulation

Source : Hawks et al. **IJBC** 2019

Results for the normal case (healthy)

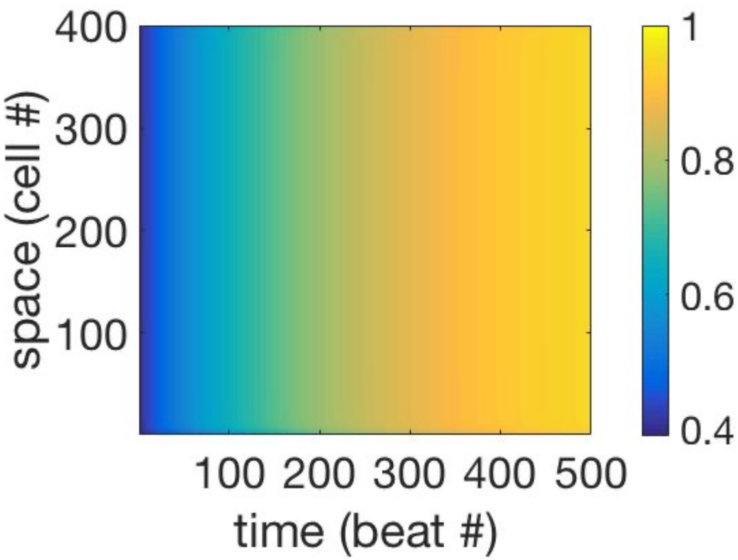

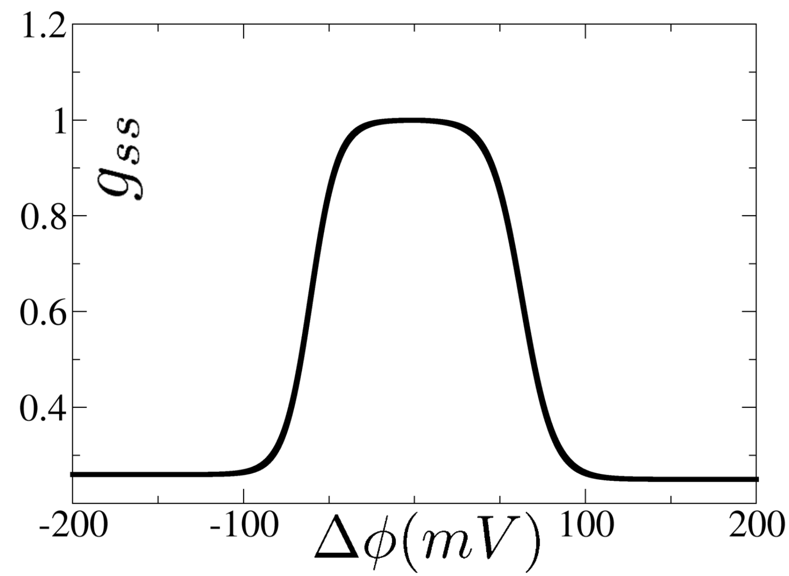

Here we set $g_{ini} = 0.4$

The conductances of all the GJ are returning to the max value $g \sim 1$

Nothing fancy happens !

Source : Hawks et al. **IJBC** 2019

Modification of the GJ dynamics (diseased case)

(Diseased)

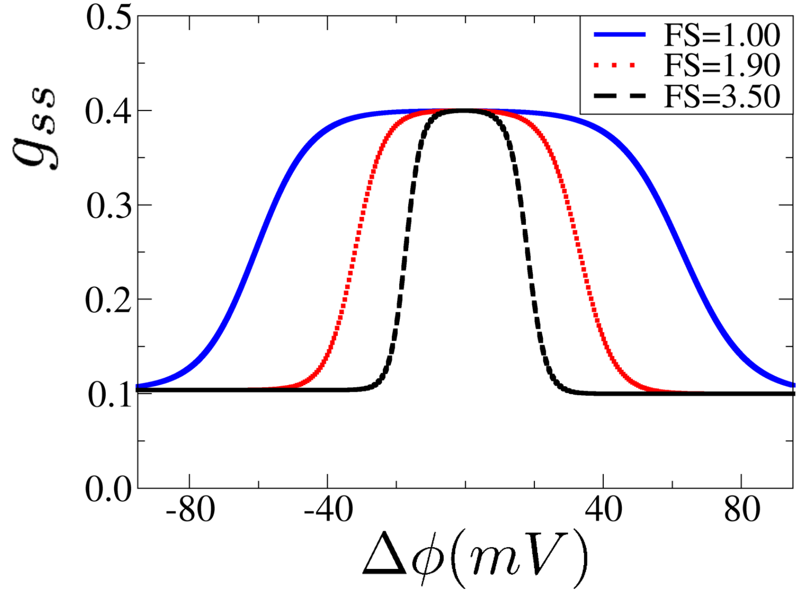

(Normal)

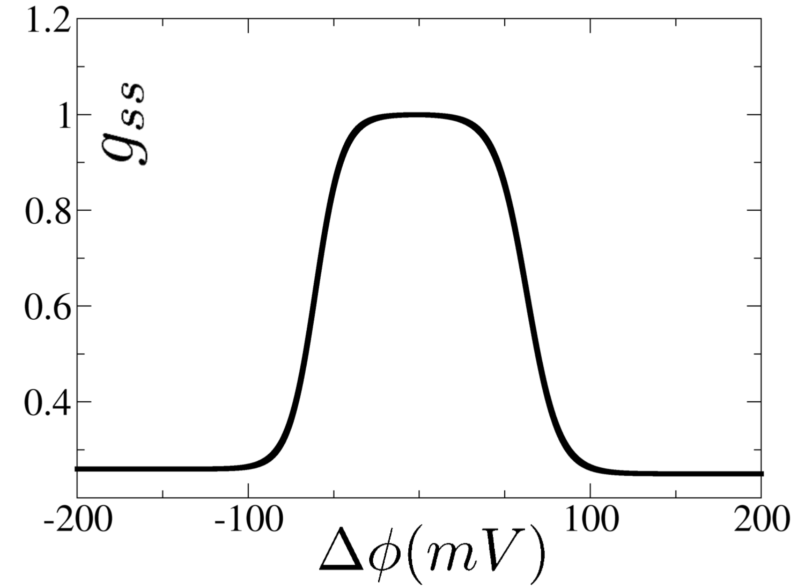

In order to model a diseased tissue we modify the characteristics of the GJ

- We reduce the overall conductance to 40% of the normal values (ischemia)
- We introduce the 'shrinking factor' FS that alters the width of the plateau

Source : Hawks et al. **IJBC** 2019

Results of the GJ bistability induced by varying FS

FS=1

FS=1.44

FS=1.9

FS=3.5

FS=20

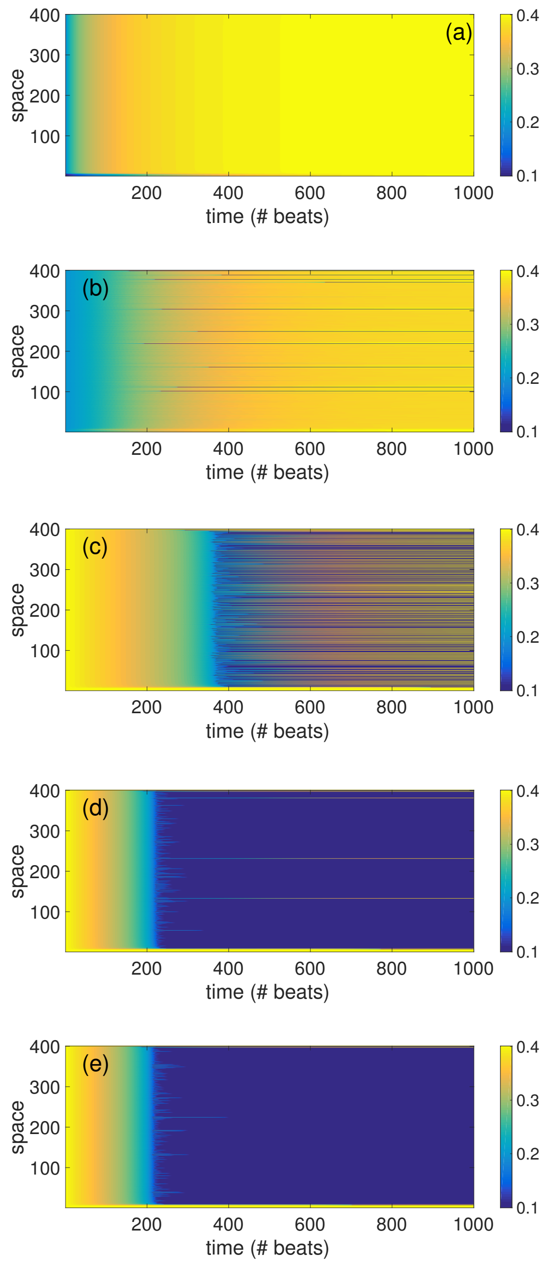

FS=1.9

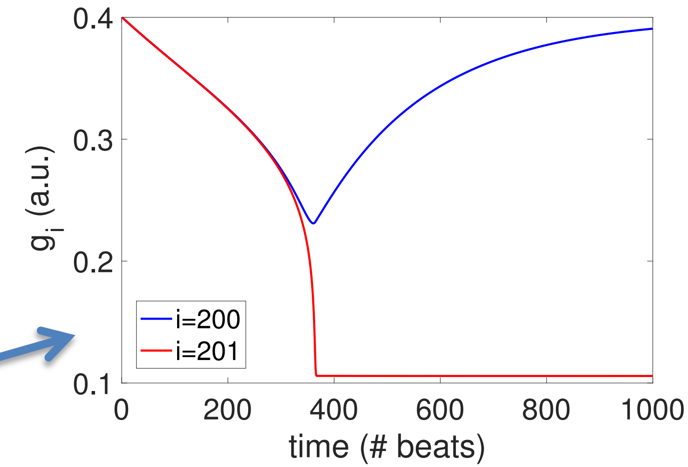

We observe a transition by increasing FS from GJ conductance close to 0.4 (upper state) to GJ conductance close to 0.1 (lower state). For intermediate values of FS, we observe a spatially mixed state.

Source : Hawks et al. **IJBC** 2019

Study of the transition from UP to LOW GJ conductances

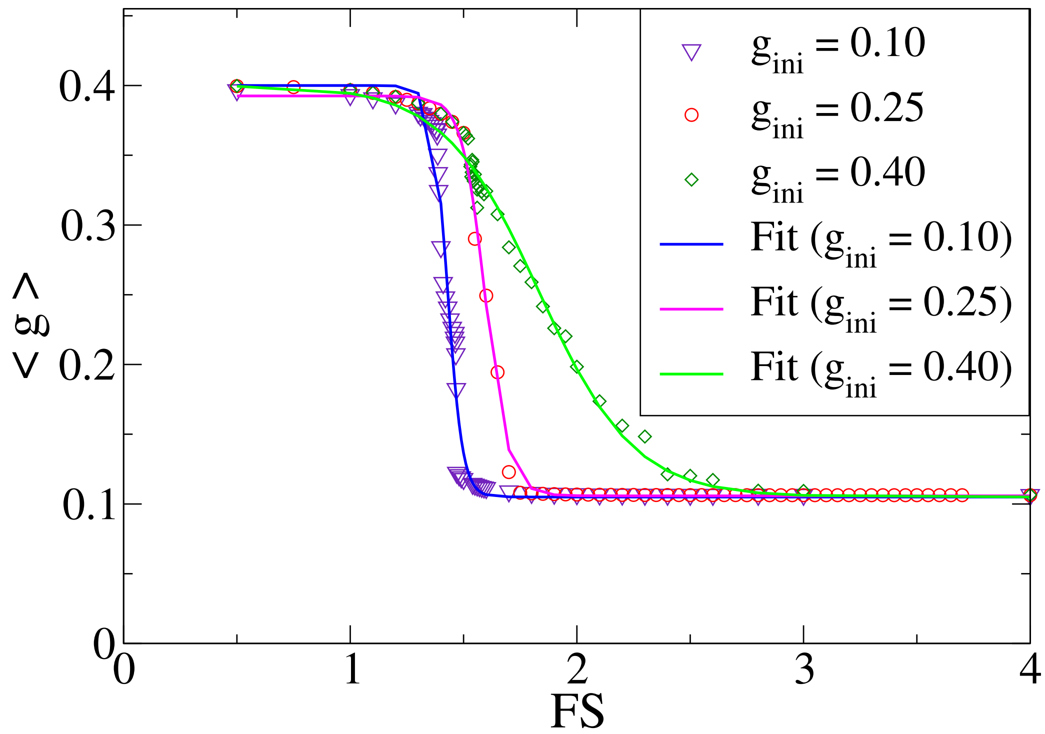

We have studied the influence of both FS and g_{ini}

for characterizing the transition between upper and lower states of conductance

The spatial average of the conductance $< g >$ is used as

an order parameter to characterize this transition

Hysteresis is observed when varying the initial values of the conductance

Influence of g_{ini} and added noise on the transition

We have studied the influence of an initial added noise $g_i^{(0)} = g_{ini} + N_s\,\sigma_u$ to the transition.

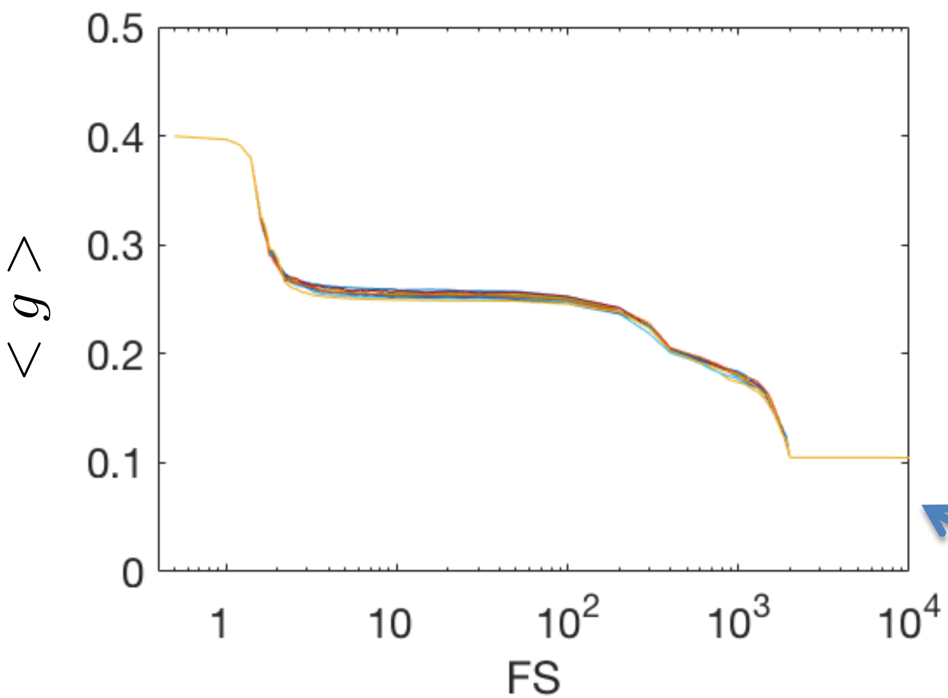

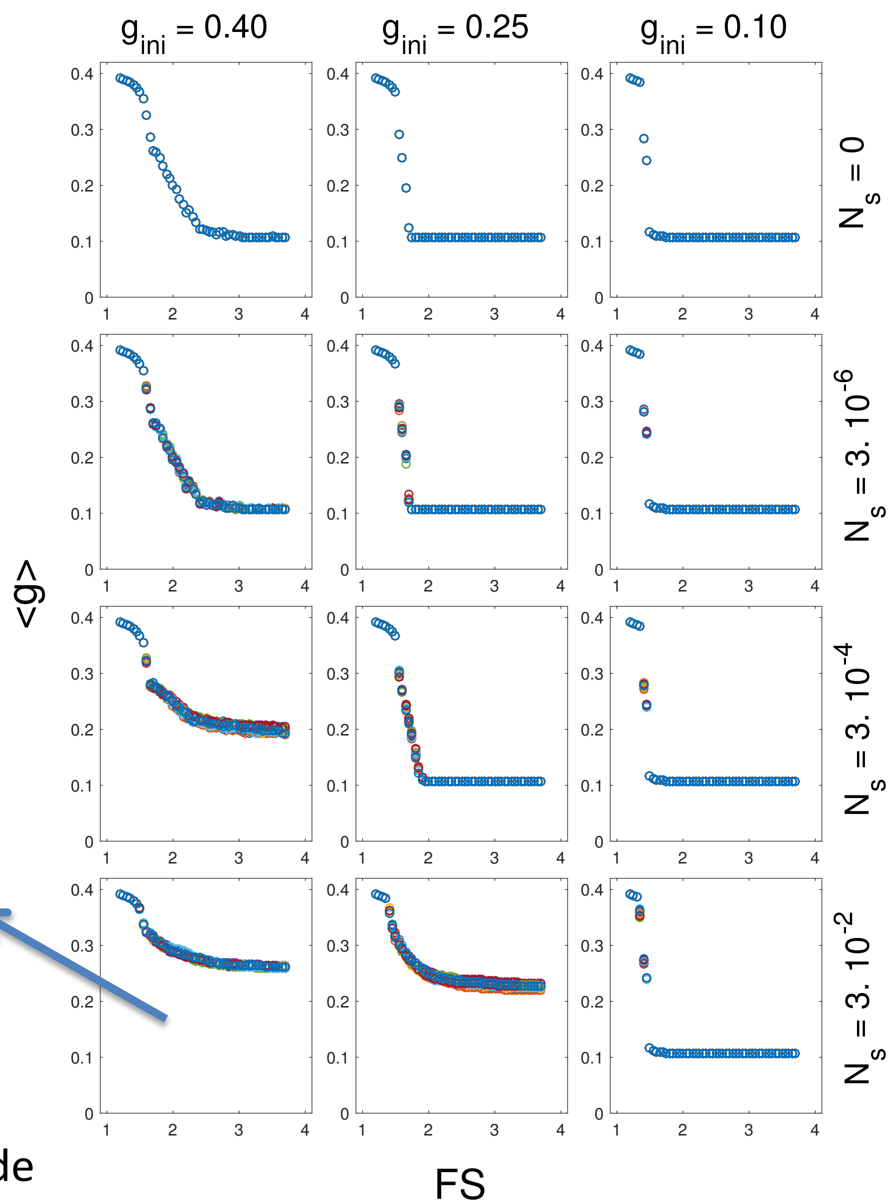

Persistent mixed state over 3 orders of magnitude

Results of the GJ bistability (Subcellular case)

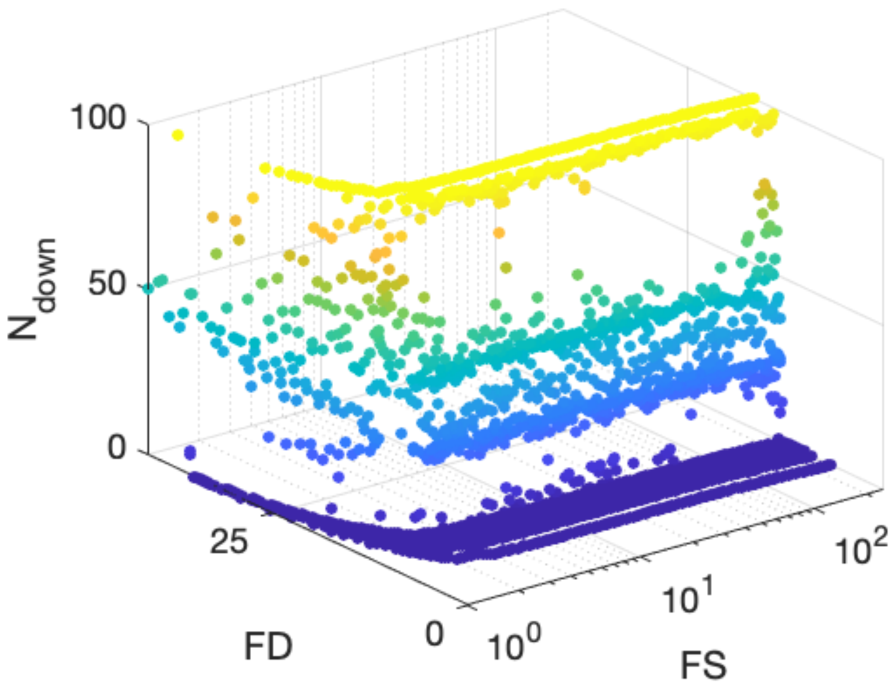

In the subcellular simulations,

we again observe the transitions for

some selected values of the

FS and FD factors.

Top View

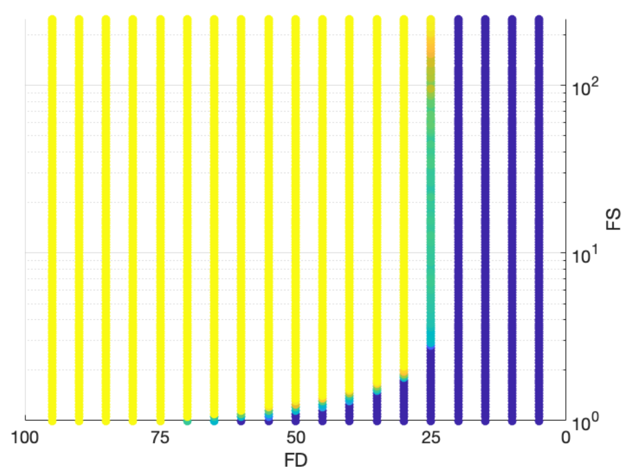

At the transition:
FD parameter has to be precise.
FS parameter variation is large.

Non-homogeneous conductance induces dispersion in the AP conduction velocity

$$c_i = \frac{\Delta x}{\Delta t_i}$$

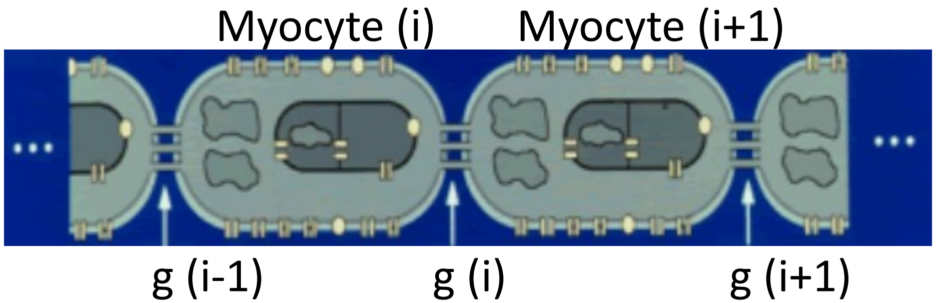

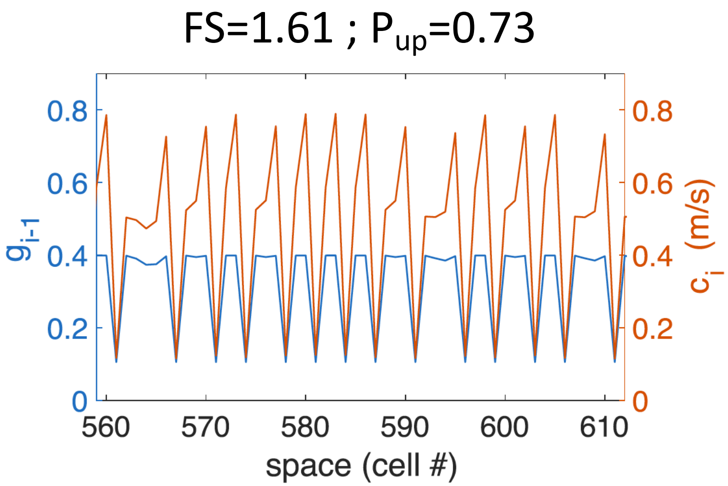

$\rho = 0.906$

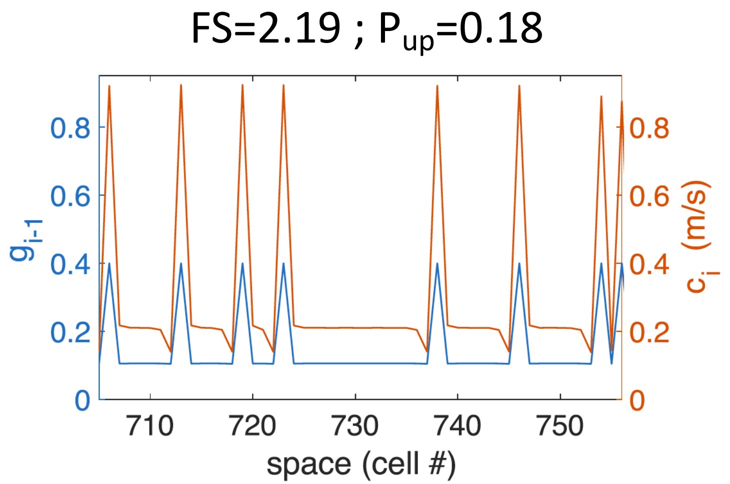

$\rho = 0.996$

- Local conductances and local conduction velocities are strongly correlated
- The relation is not strictly local !
- Propagation is from left to right !

Dispersion relations for the AP velocity

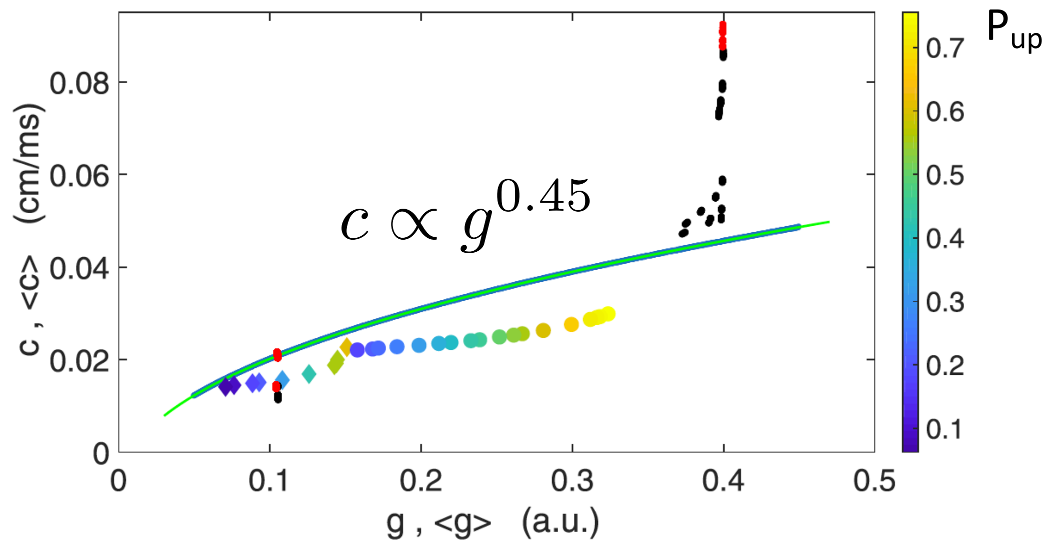

Local

↓

Non-local

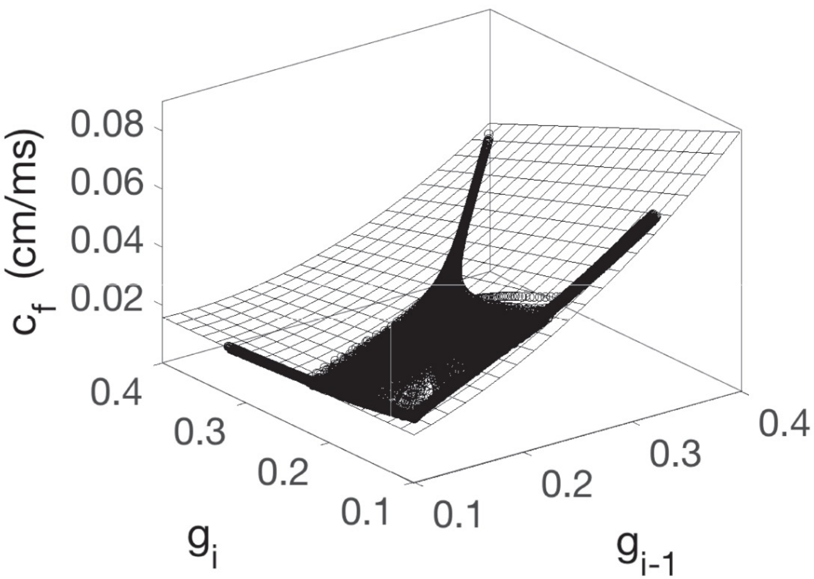

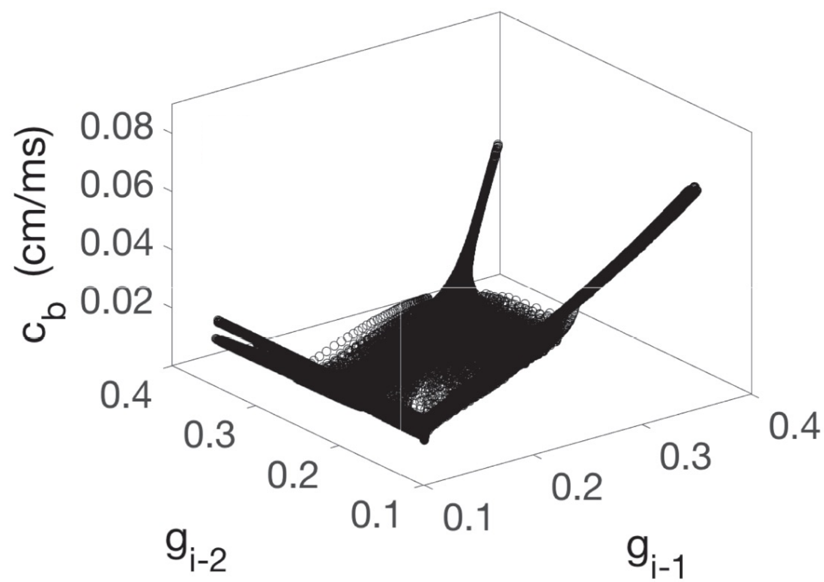

Stability of a single GJ

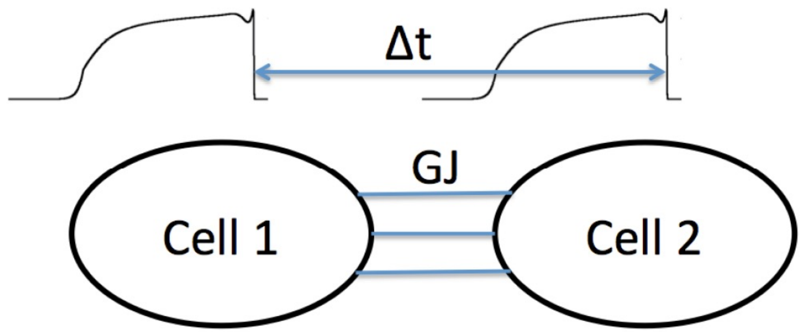

$$\frac{dg}{dt} = \frac{g_{ss}(\Delta\phi) - g}{\tau_g(\Delta\phi)}$$

Kinematic relation: $\Delta\phi = \Delta V = V|_2 - V|_1 = V(t-\Delta t) - V(t)$

$$\Delta t = \frac{\delta x}{c(g)}$$

FS=1.67

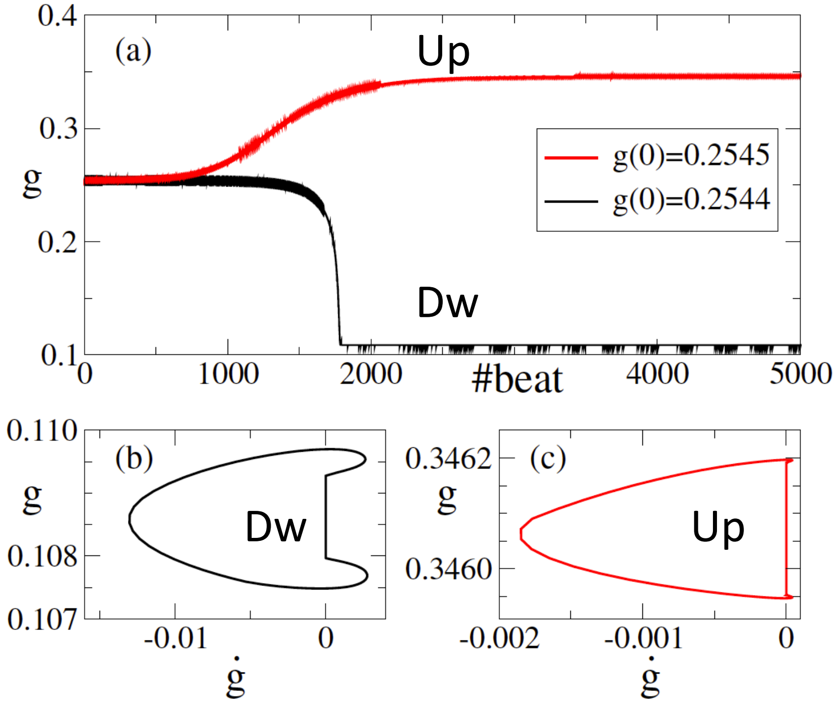

Bistability range for FS in [1.46 ; 1.72]

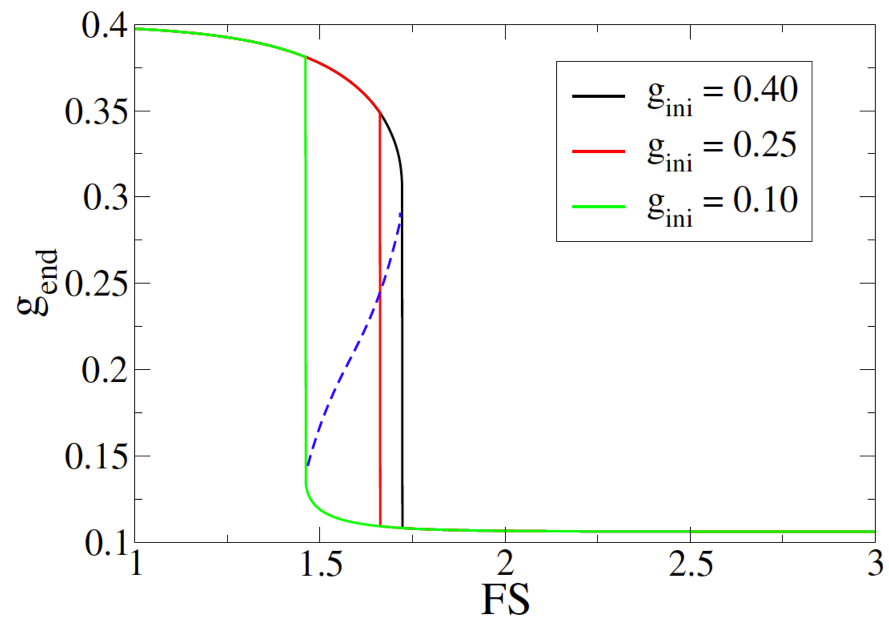

Two coupled GJs

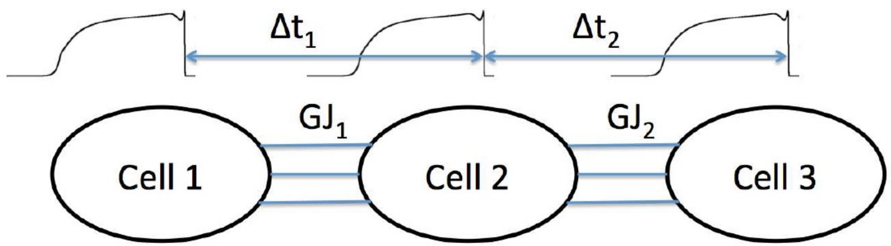

$$\begin{cases} \dfrac{dg_1}{dt} = \dfrac{g_{ss}(\Delta\phi_1) - g_1}{\tau_g(\Delta\phi_1)} \\[2ex] \dfrac{dg_2}{dt} = \dfrac{g_{ss}(\Delta\phi_2) - g_2}{\tau_g(\Delta\phi_2)} \end{cases}$$

Kinematic relations: $\Delta t_1 = \dfrac{\delta x}{c_f(g_1, g_2)}$ $\quad$ $\Delta t_2 = \dfrac{\delta x}{c_b(g_2, g_1)}$

Attractor name	End g_1	End g_2	Local stability
Dw–Dw (I)	~ 0.1	~ 0.1	$1.24 < FS$
Dw–Up (II)	~ 0.1	~ 0.4	$0.985 < FS < 993.1$
Up–Dw (III)	~ 0.4	~ 0.1	$0.985 < FS < 993.1$
Up–Up (IV)	~ 0.4	~ 0.4	$FS < 1.665$

FS=1.4

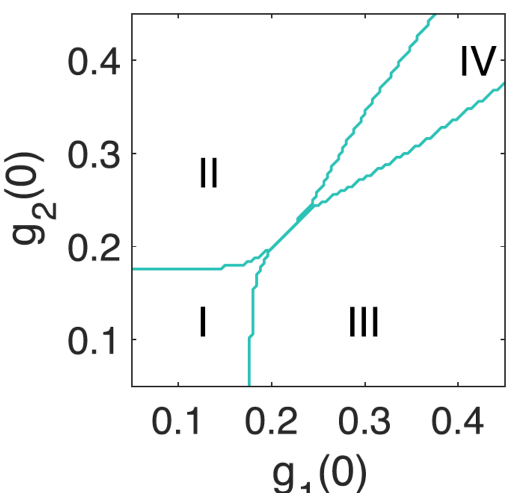

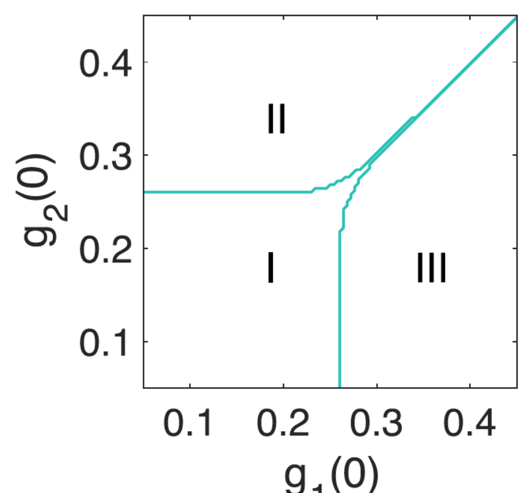

FS=500

Related experimental study showing bistability for GJ

Junctional delay, frequency, and direction-dependent uncoupling of human heterotypic Cx45/Cx43 gap junction channels

Willy G. Ye [a,1], Benny Yue [a,1], Hiroshi Aoyama [b], Nicholas K. Kim [a], John A. Cameron [a], Honghong Chen [a], Donglin Bai [a,*]

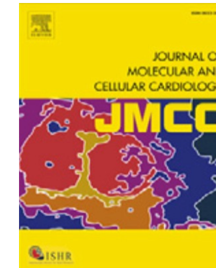

$\Delta t = 10\mathrm{ms}$

Pacing = 1Hz

Pacing = 3Hz

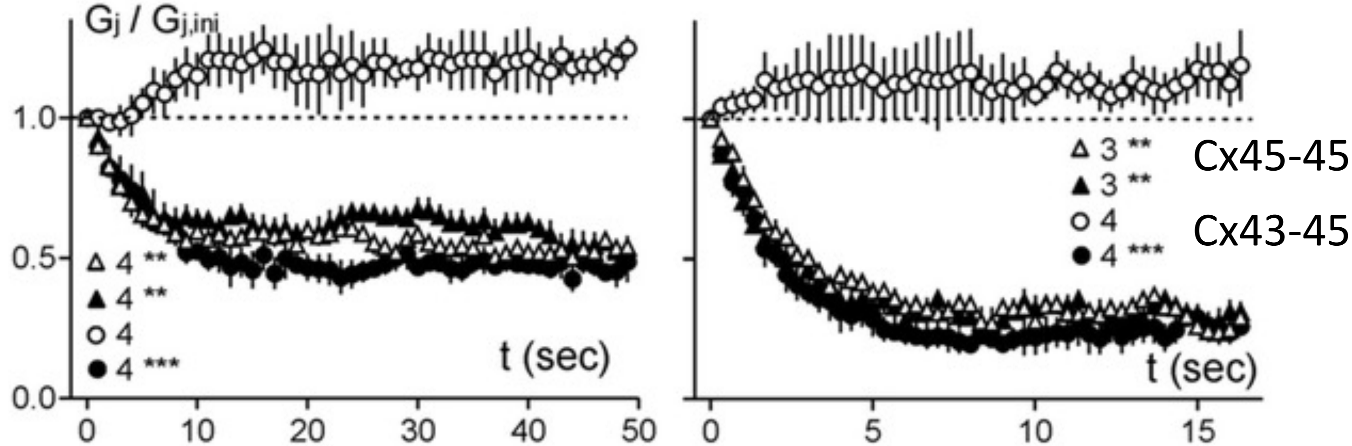

By varying the junctional delay Δt and the pacing frequency, they observe a different dynamics for the GJ conductances.

It is also highly dependent on the GJ composition.

Source : W.G. Ye et al., JMCC. **111** , 2017

Conclusions

- We have studied the conductance dynamics of the GJ in a 1D model
- In some simulated diseased situations we observe bistability in the values of the GJ conductances.
- The high to low level of conductance is mediated by parameter FS.
- In the intermediate mixed state we observe a highly alternating spatial distribution of the GJ conductances.
- A simple stability analysis of the GJ dynamics explains the observations.
- Future Plan: Connect our findings to electrophysiology experiments

J. Bragard et al., Chaos 31, 073144 (2021); doi: 10.1063/5.0053651

Acknowledgements

Collaborators:

UNAV-CIMA-CUN (Dr. Javier Diez, MD, Dr. I. Garcia-Bolao, MD, …)

UPC Barcelona (B. Echebarria, A. Peñaranda,
I.R. Cantalapiedra, E. Alvarez-Lacalle)

Liege University (P.C. Dauby, A. Collet, …)

Utah CVRTI (F.B. Sachse, A.C. Sankarankutty, …)

Max Planck Göttingen (A. Witt, S. Luther,...)

Financial support : (MINECO) under grant number PID2020-116927RB-C22
(Spain research grant)

Thank you !

Justification of the FS factor

(Diseased)

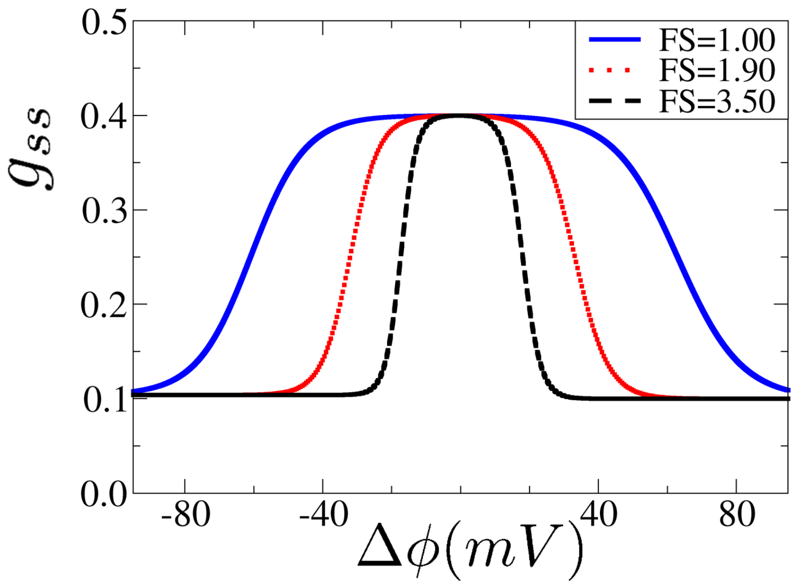

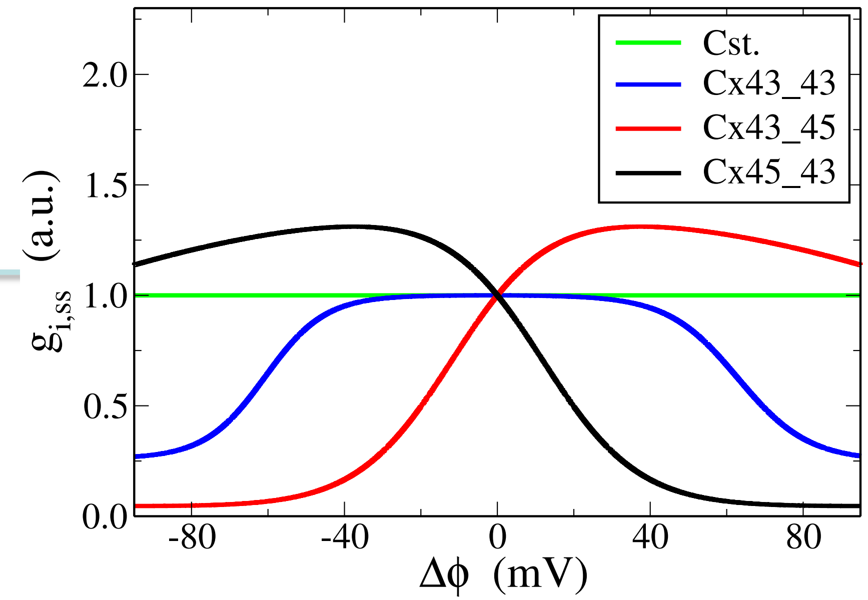

Heterotypic GJs have asymmetrical g_{ss} functions.

A mix of several type of GJ types may justify the FS parameter

Source : Hawks et al. **IJBC** 2019

Justification of the introduction of noise (Ns)

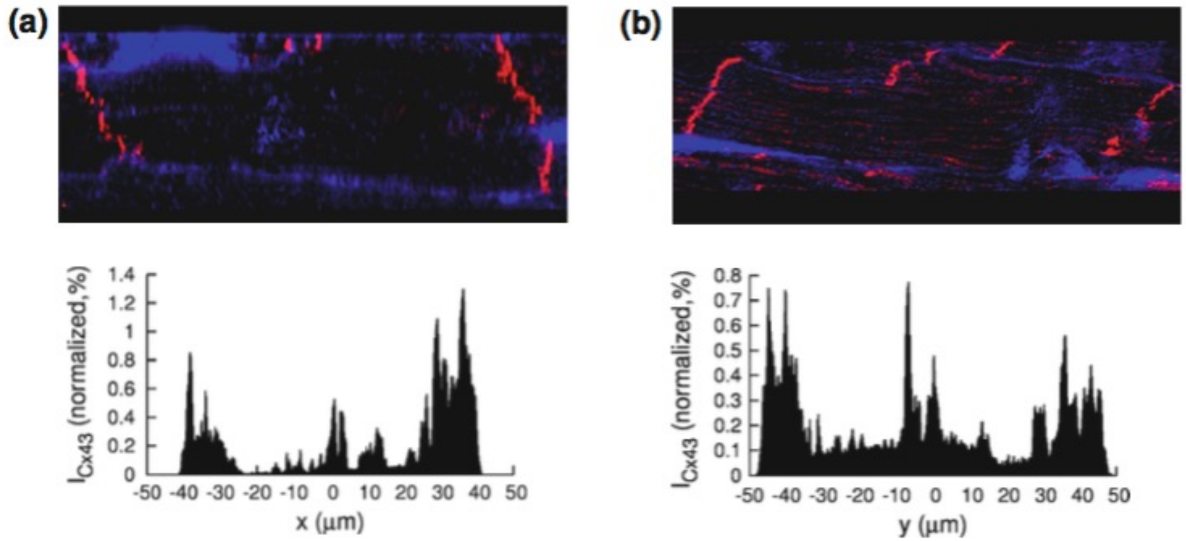

Spatial heterogeneities and different geometric orientation

lead to variability in the GJ conductance

This may justify the noise factor

Source : DP Lackey et al. **Ann. BE** 2011